Stable Single-Layer Honeycomblike Structure of Silica

V. Ongun Özçelik,[1,2] S. Cahangirov,[3,4] and S. Ciraci[4,*]
[1]UNAM-National Nanotechnology Research Center, Bilkent University, 06800 Ankara, Turkey
[2]Institute of Materials Science and Nanotechnology, Bilkent University, Ankara 06800, Turkey
[3]Nano-Bio Spectroscopy Group, Departamento Fisica de Materiales, Universidad del Pais Vasco, Centro de Fisica de Materiales CSIC-UPV/EHU-MPC and DIPC, Avenida Tolosa 72, E-20018 San Sebastian, Spain
[4]Department of Physics, Bilkent University, Ankara 06800, Turkey
(Received 7 October 2013; published 20 June 2014)

Silica or SiO_2, the main constituent of Earth's rocks has several 3D complex crystalline and amorphous phases, but it does not have a graphitelike layered structure in 3D. Our theoretical analysis and numerical calculations from the first principles predict a single-layer honeycomblike allotrope, $h\alpha$ silica, which can be viewed to be derived from the oxidation of silicene and it has intriguing atomic structure with reentrant bond angles in hexagons. It is a wide band gap semiconductor, which attains remarkable electromechanical properties showing geometrical changes under an external electric field. In particular, it is an auxetic metamaterial with a negative Poisson's ratio and has a high piezoelectric coefficient. While it can form stable bilayer and multilayer structures, its nanoribbons can show metallic or semiconducting behavior depending on their chirality. Coverage of dangling Si orbitals by foreign adatoms can attribute new functionalities to $h\alpha$ silica. In particular, Si_2O_5, where Si atoms are saturated by oxygen atoms from top and bottom sides alternatingly can undergo a structural transformation to make silicatene, another stable, single layer structure of silica.

DOI: 10.1103/PhysRevLett.112.246803 PACS numbers: 73.22.−f, 77.55.−g, 81.05.Zx, 81.07.−b

Trends in materials science have aimed at the discovery of single layer structures and their multilayer van der Waals composites by using advanced fabrication techniques [1]. In this endeavor, silicene, a graphenelike single layer honeycomb structure of silicon, was shown to be stable [2,3] and was later synthesized on Ag(111) substrate [4]. The interaction of silicene with oxygen has been a subject of active research [5–10] because it directly affects the fabrication process of silicene-based devices. Besides this, silicene-oxygen interaction leads to new two-dimensional (2D) silica crystals in different forms [5,6] and bilayer structures [11]. Recently, efforts have been devoted to grow 2D ultrathin polymorphs of silica on substrates [6,11–14], and theoretical studies have also been carried out to understand 2D silica and their defects [9,15,16]. In various 3D fourfold coordinated allotropes of SiO_2, such as amorphous and crystalline quartz, which are commonly named as silica, Si-O-Si bonds are bent around oxygen atoms [17], except for β cristobalite which has straight Si-O-Si bonds [18]. However, none of those allotropes of silica are known to have a graphenelike freestanding 2D structure or a graphitelike layered structure.

In this Letter, we predict a single layer allotrope of silica named $h\alpha$ silica (h denoting the single layer hexagonal lattice). Having passed through various complex stability tests, this honeycomblike structure is found to be stable. It has a more complex structure and exceptional properties as compared to those ultrathin films grown on substrates; it is a wide band gap semiconductor having a negative Poisson's ratio and high piezoelectric coefficient. The band gap can be reduced or widened depending on the direction of the applied uniaxial tensile stress. Even more remarkable, this basic structure, $h\alpha$ silica, can also form bilayer and multilayer structures and interact readily with adatoms like O, H, F to form a manifold of its derivatives. In particular, when Si atoms are saturated by oxygen, the resulting derivative Si_2O_5, is transformed to silicatene at elevated temperature. Our predictions are obtained from first-principles calculations, which are detailed in Refs. [19–26].

Silicene surface is rather reactive; O atoms are bonded to the bridge site with a strong binding energy of 6.17 eV [8]. This bridge bonded O adatom can forcibly switch between two bistable equilibrium positions at either side if an energy barrier of 0.28 eV is overcome [8]. At the transition state, the Si-Si bond is stretched to accommodate one O atom near its midpoint and, hence, to form a Si-O-Si bond. Then, one may contemplate whether an exothermic process can take place, in which one O atom can be inserted between each Si-Si bond of silicene concomitantly to grow a single layer honeycomblike network in 2D with the formula unit of Si_2O_3. Actually, a similar process occurs in 3D through the oxidation of silicon surfaces to generate amorphous SiO_2.

A hexagonal unit cell including two Si and three O atoms forms a regular honeycomb network, as shown in Fig. 1(a). This structure, which we named as $h\beta$ silica in analogy to β cristobalite in 3D, corresponds to a shallow local minimum. When perturbed from perfect symmetry and subsequently

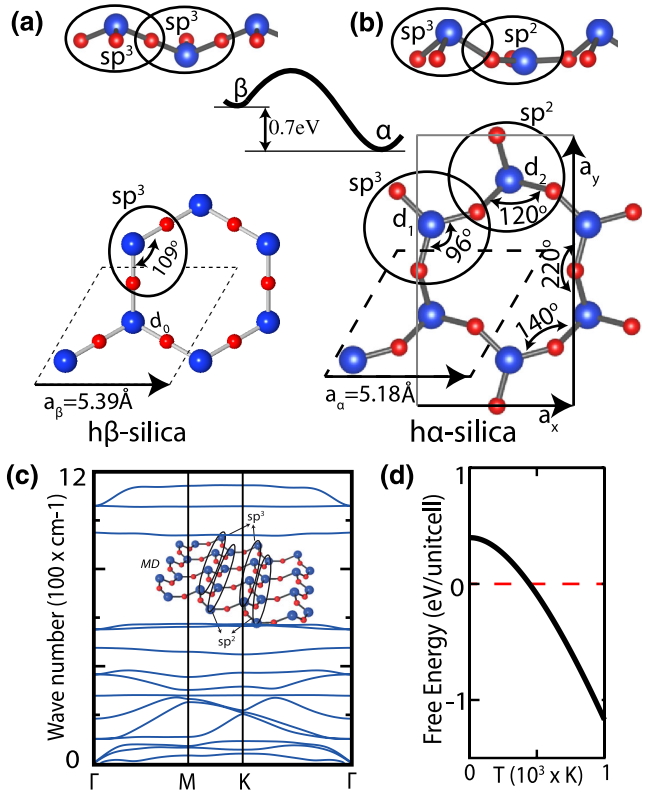

FIG. 1 (color online). (a) Side and top views of $h\beta$ silica. Large blue and small red balls stand for Si and O atoms. (b) Optimized structure of $h\alpha$ silica with its hexagonal and rectangular unit cells. Two types of Si atoms, i.e., sp^3 bonded and sp^2 bonded are indicated. (c) Calculated phonon bands and tilted view of the MD simulation in 4×4 unit cell. (d) Free energy versus temperature.

relaxed by the conjugate gradient method using stringent convergence criteria, $h\beta$ silica eventually transforms to a new structure, $h\alpha$ silica, and the energy is lowered by 0.7 eV. The optimized geometrical parameters of this allotrope and other physical properties are described in Fig. 1(b) and Table I. In the optimized structure, three alternating Si atoms of a hexagon engage in planar sp^2 bonding and the remaining three rise upward or downward [27] and form sp^3-like bonds [28]. Consequently, the rotary reflection symmetry is broken and the lattice is shrunk by ~4%. The straight Si-O-Si bonds are bent forming reentrant bond angles [29], such that all O atoms are coplanar together with the sp^2-bonded Si atoms. Thus, the regular hexagons are distorted where Si atoms are placed at the corners of hexagons, but they are buckled like silicene. Its high cohesive energy, $E_c = 28.6$ eV per unit cell originates from mixed (covalent and ionic) bonds between Si and O atoms while its high formation energy prevents it from clustering. These rearrangements are reminiscent of the transition from ideal β cristobalite to α quartz in 3D.

The rigorous answer to the question of whether the optimized structure is stable is provided by calculating the phonon frequencies with extreme accuracy. All frequencies of the infinitely large, single layer are found to be positive in the first Brillouin zone. As shown in Fig. 1(c), the calculated bands of frequencies, $\Omega(\mathbf{k})$, with a minute gap between optical and acoustical branches, clearly demonstrate that $h\alpha$ silica remains stable even if the stabilizing finite size and edge effects are absent. Otherwise, the specific eigenfrequencies of the dynamical matrix would be imaginary if any instability due to the long wavelength transversal acoustical phonons was imposed.

Although the phonon spectrum provides supports that $h\alpha$ silica is a local energy minimum, we further examine the thermodynamic stability by calculating the variation of free energy with temperature. Our results that are derived from the phonon calculations, including the entropy part, indicated in Fig. 1(d) that the system has positive free energy up to 500 K.

To further investigate the effects of temperature on stability, we perform *ab initio* molecular dynamics (MD) calculations at high temperatures. Since a small unit cell may easily lead to fake instability, we used a relatively large (4×4) supercell. Starting from regular $h\beta$ silica, and by raising the temperature to 1000 K, the structure has transformed to $h\alpha$ silica and did not change in the course of MD simulations lasting 12 ps as shown by the inset of Fig. 1(c). No instability leading to structural transformation or dissociation of $h\alpha$ silica was observed even if the specific phonon modes were softened at such a high temperature. Additionally, through intermediate energy paths, specific atoms were displaced forcibly from their optimized local equilibrium positions corresponding to a minimum in the Born-Oppenheimer surface. The optimized structure was resistant to these deformations and, hence, restored itself quickly. This situation demonstrates that the minimum is

TABLE I. Relevant physical properties of $h\alpha$ silica. a_α: hexagonal lattice constant in Å; d_1: Si-O bond distance of sp^3-bonded Si; d_2: same for sp^2-bonded Si; t: perpendicular distance between sp^3-bonded and sp^2-bonded Si atoms in Å; E_c, E_f: the cohesive and formation energies per unit cell in eV; $E_{G-\mathrm{GGA}}$: band gap calculated by generalized gradient approximation (GGA) with van der Waals correction in eV; $E_{G-\mathrm{HSE}}$: band gap calculated by Heyd-Scuseria-Ernzerhof (HSE); C: in-plane stiffness in N/m; ν: Poisson ratio; Q^*_O, $Q^*_{Si-sp^3}$, $Q^*_{Si-sp^2}$: Mulliken charges in electrons for different atoms.

a_α	d_1	d_2	t	E_c	E_f	$E_{G-\mathrm{GGA}}$	$E_{G-\mathrm{HSE}}$	C	ν	Q^*_O	$Q^*_{Si-sp^3}$	$Q^*_{Si-sp^2}$
5.18	1.76	1.58	0.96	28.6	9.2	2.2	3.3	22.6	-0.21	−0.31	0.53	0.39

deep enough to retain the structure of $h\alpha$ silica stable at ambient conditions.

Our conclusions on the mechanical stability is corroborated further by calculating its in-plane stiffness, $C = A_o^{-1}\partial^2 E_T/\partial\epsilon^2$ (in terms of the area A_o of the cell and the variation of total energy, E_T with strain, ϵ). Here, calculations can conveniently be performed in a rectangular cell by applying uniaxial strain along x and y directions to deduce that $C_x \simeq C_y = 22.6$ J/m^2. The calculated in-plane stiffness is smaller than that of graphene [30].

The Poisson's ratio $\nu = -\epsilon_y/\epsilon_x$, is calculated as $\nu = -0.21$. This is remarkable in the sense that, as $h\alpha$ silica is stretched along the x direction, it also expands in the y direction, owing to its squeezed structure consisting of twisted and bent Si-O-Si bonds. Thus, three oxygen atoms in each hexagon protrude inward resulting in a reentrant structure [29]. The negative Poisson's ratio is a rare situation [31] and is also observed in foams produced from low density, open-cell polymers [32,33]. These extremal materials, also called auxetics or metamaterials, offer crucial applications for biotechnology and nanosensors.

Electronic properties of $h\alpha$ silica are summarized in Fig. 2, which shows that it is a nonmagnetic, wide band gap semiconductor with a direct band gap of $E_{G-\mathrm{GGA}} = 2.2$ eV predicted using GGA calculations [23]. When corrected by HSE [24], the gap increases to $E_{G-\mathrm{HSE}} = 3.3$ eV. While conduction and valance band edges are mainly derived from the dangling orbitals of sp^2-bonded and sp^3-bonded Si, respectively, the bands of oxygen-p orbitals occur below ~ -4 eV.

According to Mulliken charge analysis [26] summarized in Fig. 2(b), Si-O bonds have a strong ionic character. Because of the special bond configuration, each oxygen atom receives ~0.31 excess electrons, while 0.53 electrons and 0.39 electrons are donated by sp^3- and sp^2-bonded Si atoms, respectively. The details of charge transfer are depicted by charge density isosurfaces and contour plots. Charge rearrangements are also reflected by the calculated total charge density in Fig. 2(c), where oxygen and corner Si atoms are seen by bright and dispersed spots, respectively, while sp^3-bonded Si atoms are not seen. Because of the significant charge transfer between Si and O atoms, dipole moments along x and y directions are expected to be high.

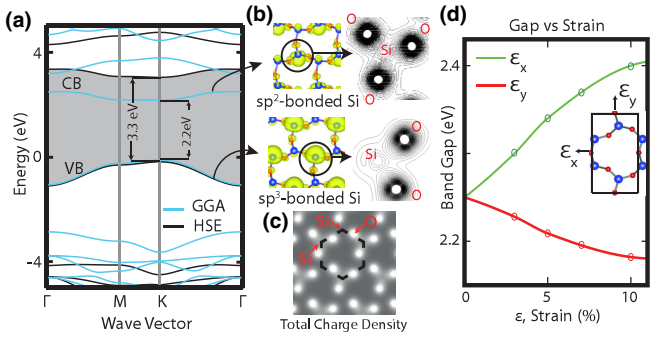

FIG. 2 (color online). (a) The electronic band structure of $h\alpha$ silica. (b) Isosurface charge densities of the lowest conduction (CB) and highest valence (VB) band, and contour plots of the total charge density in the planes of O-Si-O for the sp^2- and the sp^3-bonded Si atoms. (c) Images of the total charge density. (d) Variation of the band gap as a function of the uniaxial strains ϵ_x and ϵ_y.

It is a rather rare situation that the variation of the calculated band gap is strain specific; it increases with increasing uniaxial strain, ϵ_x, but it decreases with increasing ϵ_y as shown in Fig. 2(d). Reversed responses of the band gap to the orthogonal uniaxial tensile stresses are closely related to the atomic configuration in the rectangular unit cell described in Fig. 1.

Nanoribbons attribute further relevance to $h\alpha$ silica. In Fig. 3, we consider zigzag and armchair nanoribbons specified by the number of hexagons across their widths w, $N_Z = 4$ and $N_A = 4$, respectively. Apart from the minute reconstruction at their edges, these nanoribbons are stable. The zigzag $N_Z = 4$ nanoribbon is a metal, where the flat band at the Fermi level is derived from the orbitals of sp^2-bonded atoms located at one edge. Another band crossing the Fermi level has small dispersion and originates from the orbitals of sp^3-bonded Si atoms at the other edge. In contrast, the armchair nanoribbon is a semiconductor with a direct band gap of 1.9 eV calculated within GGA [23]. The bands at the conduction and valance band edges are derived from the sp^2-bonded and sp^3-bonded Si atoms at both edges, respectively. Because of small coupling between edges, the bands are slightly split. These nanoribbons with or without foreign adatoms attached to the edges and their networks consisting of the combination of zigzag and armchair nanoribbons with different N_Z and N_A, can display a diversity of electronic properties, which is beyond the scope of the present study. Here, we point out a property of $h\alpha$ silica, which may be of potential importance. Because of the significant charge transfer between Si

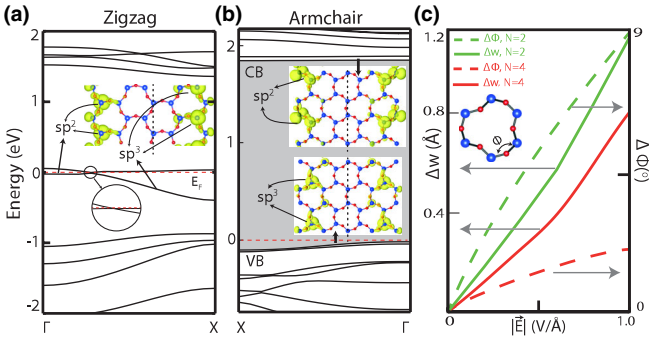

FIG. 3 (color online). (a) Electronic band structure of zigzag nanoribbon with $N_Z = 4$. (b) Same for the armchair nanoribbon with $N_A = 4$. (c) Variation of the width of the armchair nanoribbon Δw and bond angle $\Delta\phi$ under an in-plane electric field $\vec{E}$ applied perpendicular to the axis.

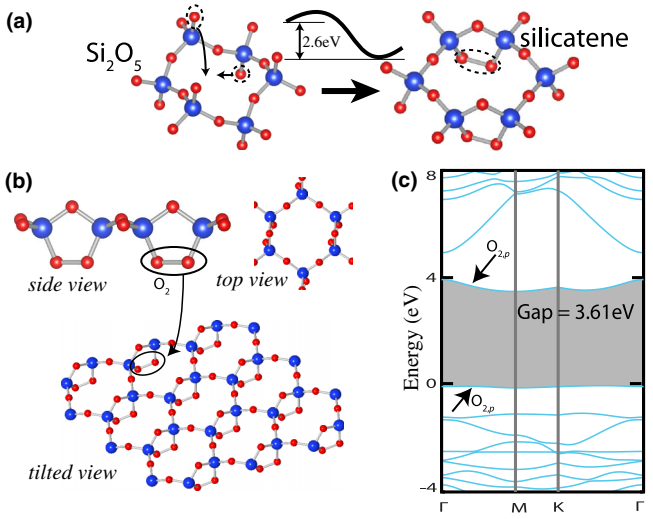

FIG. 4 (color online). (a) Silicatene derived from Si_2O_5. (b) Atomic structure of silicatene with side, top, and tilted views. Pentagons are formed from three O and two Si atoms. (c) Electronic band structure. Bands derived from O-O bonds are indicated.

and O atoms and its reentrant structure, a finite size flake of $h\alpha$ silica is expected to be influenced by the applied electric field. The effect of the in-plane electric field, $\vec{E}$, is investigated on the armchair nanoribbons. As illustrated in Fig. 3(c), an applied in-plane electric field induces significant changes in the width Δw and Si-O-Si bond angle ϕ of armchair nanoribbons. The piezoelectric coefficient is estimated from Δw as 5.7×10^{-12} m/V, which is more than twice the value measured for quartz [34], which is crucial for piezoelectric nanodevices.

It should be noted that the basic structure of $h\alpha$ silica and its ribbons discussed so far are reactive due to dangling bonds or π orbitals oozing from Si atoms. Thus, they can acquire new functionalities by the adsorption of adatoms to Si, such as H, F, O, etc. Like graphene, uniform and full coverage of $h\alpha$ silica by one of these atoms can produce new derivatives $Si_2O_3H_2$, $Si_2O_3F_2$, and Si_2O_5. A summary of the properties attained by these derivatives, as well as bilayer and multilayer structures are presented in the Supplemental Material [35]. Here, the derivative Si_2O_5 is of particular interest. Upon oxidation through the saturation of Si dangling bonds alternating from the top and bottom sides, the filled band at the top of the valance band derived from the orbitals of sp^3-bonded Si and the empty band at the bottom of the conduction band derived from the orbitals of sp^2-bonded Si atoms in Fig. 2 are removed and the band gap increases from 2.2 eV to ~6 eV, attributing a high insulating character and inertness like 3D silica. While the hexagonlike 2D geometry in Fig. 1 is maintained, sp^2-bonded Si atoms change to sp^3-bonded Si atoms and, hence, restore the rotary reflection symmetry. This way, Si atoms acquire the fourfold coordination of oxygen atoms in Fig. 4(a) as in 3D silica. However, upon heating, Si_2O_5 undergoes a structural transformation by further lowering (i.e., becoming more energetic) its total energy by 2.63 eV, whereby the first half of the dangling Si-O bonds rotate from top to bottom so that all are relocated at the bottom side. Eventually, they are paired to form O-O bonds as shown in Fig. 4(a). The resulting electronic structure of this phase is presented in Fig. 4(b). The filled and empty bands occurring in the band gap of Si_2O_5 are derived from O-O bonds. As a final remark, it is gratifying that the optimized atomic structure predicted in Fig. 4(a) replicates the structure of the single layer silica in a honeycomb structure (named silicatene), the growth of which was achieved recently on a Ru(0001) surface [36]. The measured lattice parameters also agree with the present calculated values. Based on the present analysis, it is revealed that silicatene is bonded to metal substrates through O-O bonds below the Si plane.

In conclusion, we showed that the single layer honeycomblike structure of silica, $h\alpha$ silica, is stable and mimics the well-known crystalline quartz in 2D. Additionally, this allotrope and its nanoribbons display exceptional electromechanical properties and can attain bilayer and multilayers through the stacking of silica single layers. While diverse functionalities can be attained by the adsorption of foreign atoms, a new phase named silicatene forms when the dangling Si orbitals are saturated by oxygen atoms. While the allotropes of bulk silica have made a great impact in fundamental and applied research, the exceptional properties revealed in this Letter herald that $h\alpha$ silica and its derivatives can present potential applications, such as composite materials, functional coatings, and also, as single layer insulators in nanoelectronics and nanocapacitors.

The computational resources have been provided by TUBITAK ULAKBIM, High Performance and Grid Computing Center (TR-Grid e-Infrastructure) and UYBHM at Istanbul Technical University through Grant No. 2-024-2007. This work was partially supported by the Academy of Sciences of Turkey (TUBA). S. Cahangirov acknowledges Marie Curie Grant No. FP7-PEOPLE-2013-IEF, project ID 628876, and Grupos Consolidados UPV/EHU del Gobierno Vasco (Grant No. IT578-13).

*ciraci@fen.bilkent.edu.tr

[1] A. K. Geim and I. V. Grigorieva, Nature (London) **499**, 419 (2013).

[2] S. Cahangirov, M. Topsakal, E. Akturk, H. Sahin, and S. Ciraci, Phys. Rev. Lett. **102**, 236804 (2009).

[3] The fact that the free standing graphene does exist, but not silicene, cannot be taken as a counter argument against the stability of silicene. All single layer structures, including graphene, need a suitable substrate if they are growing from constituent atoms. Free standing silicene does not exist,

since there is no 3D allotrope of silicon consisting of weakly bonded layers like graphite, BN, or MoS_2

[4] P. Vogt, P. DePadova, C. Quaresima, J. Avila, E. Frantzeskakis, M. C. Asensio, A. Resta, B. Ealet, and G. Le Lay, Phys. Rev. Lett. **108**, 155501 (2012).

[5] J. Weissenrieder, S. Kaya, J.-L. Lu, H.-J. Gao, S. Shaikhutdinov, H.-J. Freund, M. Sierka, T. K. Todorova, and J. Sauer, Phys. Rev. Lett. **95**, 076103 (2005).

[6] D. Loffer, J. J. Uhlrich, M. Baron, B. Yang, X. Yu, L. Lichtenstein, L. Heinke, C. Buchner, M. Heyde, S. Shaikhutdinov, H. J. Freund, R. Wlodarczyk, M. Sierka, and J. Sauer, Phys. Rev. Lett. **105**, 146104 (2010).

[7] P. De Padova, C. Quaresima, B. Olivieri, P. Perfetti, and G. Le Lay, J. Phys. D **44**, 312001 (2011).

[8] V. O. Özçelik and S. Ciraci, J. Phys. Chem. C **117**, 26305 (2013).

[9] R. Wang, X. Pi, Z. Ni, Y. Liu, S. Lin, M. Xu, and D. Yang, Sci. Rep. **3**, 3507 (2013).

[10] A. Molle, C. Grazianetti, D. Chiappe, E. Cinquanta, E. Cianci, G. Tallarida, and M. Fanciulli, Adv. Funct. Mater. **23**, 4340 (2013).

[11] P. Y. Huang, S. Kurasch, A. Srivastava, V. Skakalova, J. Kotakoski, A. V. Krasheninnikov, R. Hovden, Q. Mao, J. C. Meyer, J. Smet, D. A. Muller, and U. Kaiser, Nano Lett. **12**, 1081 (2012).

[12] T. K. Todorova, M. Sierka, J. Sauer, S. Kaya, J. Weissenrieder, J. L. Lu, H. J. Gao, S. Shaikhutdinov, and H. J. Freund, Phys. Rev. B **73**, 165414 (2006).

[13] J. Seifert, D. Blauth, and H. Winter, Phys. Rev. Lett. **103**, 017601 (2009).

[14] S. Shaikhutdinov and H-J. Freund, Adv. Mater. **25**, 49 (2013).

[15] T. Bjorkman, S. Kurasch, O. Lehtinen, J. Kotakoski, O. V. Yazyev, A. Srivastava, V. Skakalova, J. H. Smet, U. Kaiser, and A. V. Krasheninnikov, Sci. Rep. **3**, 3482 (2013).

[16] M. Durandurdu, Phys. Rev. B **81**, 174107 (2010).

[17] R. Martonak, D. Danadio, A. R. Oganov, and M. Parinello, Nat. Mater. **5**, 623 (2006).

[18] S. Ciraci and I. P. Batra, Phys. Rev. B **15**, 4923 (1977).

[19] We performed spin polarized density functional theory calculations within GGA including van der Waals corrections [20,21]. We used projector-augmented wave potentials [22] and the exchange-correlation potential is approximated with the PBE functional [23]. The Brillouin zone was sampled by $(17 \times 17 \times 1)$ **k** points in the Monkhorst-Pack scheme. Energy convergence value between two steps was chosen as 10^{-6} eV. A maximum force less than 0.001 eV/Å, and pressure less than 0.08 kPa in the unit cell was allowed. Energy band structure calculated by GGA [23] has been corrected using the HSE [24] functional. Phonon dispersions are determined using the small displacement method [25]. Dipole corrections are applied to remove spurious dipole interactions between periodic images. Effective charges on atoms are calculated in terms of atomic orbitals using the SIESTA [26] code. Structure optimizations are repeated using a (4×4) supercell to circumvent the constraints. *Ab initio* molecular dynamics calculations using the Nose thermostat were performed with a time step of 2.5 fs lasting for 12 ps. Atomic velocities were renormalized to the temperatures set at T = 1000 K at every 40 time steps.

[20] S. Grimme, J. Comput. Chem. **27**, 1787 (2006).

[21] G. Kresse and J. Furthmuller, Phys. Rev. B **54**, 11169 (1996).

[22] P. E. Blochl, Phys. Rev. B **50**, 17953 (1994).

[23] J. P. Perdew, K. Burke, and M. Ernzerhof, Phys. Rev. Lett. **77**, 3865 (1996).

[24] J. Heyd, G. E. Scuseria, and M. Ernzerhof, J. Chem. Phys. **118**, 8207 (2003); J. Paier, M. Marsman, K. Hummer, G. Kresse, I. C. Gerber, and J. G. Angyan, J. Chem. Phys. **124**, 154709 (2006).

[25] D. Alfe, Comput. Phys. Commun. **180**, 2622 (2009).

[26] J. M. Soler, E. Artacho, J. D. Gale, A. Garcia, J. Junquera, P. Ordejon, and D. Sanchez-Portal, J. Phys. Condens. Matter **14**, 2745 (2002).

[27] From the symmetry point of view it is equally probable that sp^3-bonded Si atoms can be either at the top or bottom side of the plane of oxygen atoms. This implies frustration and may lead to domain structure.

[28] Even though the bond angle of sp^3-hybrid bonds deviate from tetrahedral angles, we continue to specify related Si atoms as sp^3-bonded Si atoms throughout the text.

[29] The Si-O-Si angles between sp^2- and sp^3-bonded Si atoms, which are denoted by ϕ for oxygens protruding outward and by ϕ' for oxygen atoms protruding inward, are 140° and 220°, respectively.

[30] H. Sahin, S. Cahangirov, M. Topsakal, E. Bekaroglu, E. Akturk, R. T. Senger, and S. Ciraci, Phys. Rev. B **80**, 155453 (2009).

[31] In Ref. [30], the calculated Poisson's ratio of more than 20 stable, single layer honeycomb structures of Group IV elements and Group III–V compounds were found to be positive.

[32] R. S. Lakes, Science **235**, 1038 (1987).

[33] X. F. Wang, T. E. Jones, W. Li, and Y. C. Zhou, Phys. Rev. B **85**, 134108 (2012).

[34] V. E. Bottom, J. Appl. Phys. **41**, 3941 (1970).

[35] See Supplemental Material at http://link.aps.org/supplemental/10.1103/PhysRevLett.112.246803 for additional information about bilayer, multilayer, hydrogenated, oxygenated, and fluorinated silica.

[36] B. Yang, J. A. Boscoboinik, X. Yu, S. Shaikhutdinov, and H. J. Freund, Nano Lett. **13**, 4422 (2013).